eng

MDPI

Article

Artificial Intelligence-Based Techniques for Fouling Resistance Estimation of Shell and Tube Heat Exchanger: Cascaded Forward and Recurrent Models

Ikram Kouidri [1], Abdennasser Dahmani [2,3], Furizal Furizal [4,5], Alfian Ma'arif [6], Ahmed A. Mostfa [7], Abdeltif Amrane [8,*], Lotfi Mouni [9] and Abdel-Nasser Sharkawy [10,11]

1 GIDD Industrial Engineering and Sustainable Development Laboratory, Department of Mechanical Engineering, Faculty of Science and Technology, University of Relizane, Bourmadia 48000, Algeria; ikramkouidri295@gmail.com
2 Department of Mechanical Engineering, Faculty of Applied Sciences, University of Bouira, Bouira 10000, Algeria; dahmaniabdennasser@gmail.com
3 Laboratory of Biomaterials and Transport Phenomena (LBMPT), University of Medea, Medea 26000, Algeria
4 Department of Research and Development, Peneliti Teknologi Teknik Indonesia, Sleman 55281, Indonesia; furizal.id@gmail.com
5 Department of Informatics Engineering, Universitas Islam Riau, Pekanbaru 28284, Indonesia
6 Department of Electrical Engineering, Universitas Ahmad Dahlan, Yogyakarta 55191, Indonesia; alfianmaarif@ee.uad.ac.id
7 Department of Computer Science, University of Al-Hamdaniya, Nineveh 41006, Iraq; mostfa@uohamdaniya.edu.iq
8 Univ Rennes, Ecole Nationale Supérieure de Chimie de Rennes, CNRS, ISCR—UMR6226, F-35000 Rennes, France
9 Laboratoire de Gestion et Valorisation des Ressources Naturelles et Assurance Qualité, Faculté SNVST, Université de Bouira, Bouira 10000, Algeria; l.mouni@univ-bouira.dz
10 Mechanical Engineering Department, Faculty of Engineering, South Valley University, Qena 83523, Egypt; eng.abdelnassersharkawy@gmail.com or abdelnassersharkawy@eng.svu.edu.eg
11 Mechanical Engineering Department, College of Engineering, Fahad Bin Sultan University, Tabuk 47721, Saudi Arabia
* Correspondence: abdeltif.amrane@univ-rennes.fr

Abstract: Heat exchangers play a crucial role in transferring heat between two mediums, directly impacting energy efficiency, product quality, and operational safety in industrial systems. This study presents a novel approach for fouling resistance estimation using two artificial intelligence models, the cascaded forward network (CFN) and the recurrent neural network (RN), with a minimal set of six input parameters. The proposed models utilize temperature and flow sensor data from heat exchangers to predict fouling resistance. The training process is optimized using the Levenberg–Marquardt (LM) algorithm, ensuring rapid convergence and high accuracy. Model performance is assessed based on mean squared error (MSE), regression values (R), and statistical error analysis. The results demonstrate that both models achieve high accuracy in predicting fouling resistance, with the CFN model outperforming the RN model. The CFN model achieves an MSE of 1.54×10^{-8}, significantly lower than the RN model (MSE = 3.05×10^{-8}), resulting in a 49.5% improvement in accuracy. Additionally, statistical analysis, including error histograms and correlation analysis, further confirms the robustness of the proposed models. Compared to traditional methods, the proposed AI-based models reduce computational complexity while maintaining superior accuracy. This study highlights the potential of AI in predictive maintenance and industrial optimization, paving the way for future enhancements in intelligent fouling estimation systems.

Keywords: heat exchanger; fouling resistance; cascaded forward network; recurrent network; statistical analysis; predictive maintenance

check for updates

Academic Editor: Juvenal Rodriguez-Resendiz

Received: 11 February 2025
Revised: 7 April 2025
Accepted: 21 April 2025
Published: 24 April 2025

Citation: Kouidri, I.; Dahmani, A.; Furizal, F.; Ma'arif, A.; Mostfa, A.A.; Amrane, A.; Mouni, L.; Sharkawy, A.-N. Artificial Intelligence-Based Techniques for Fouling Resistance Estimation of Shell and Tube Heat Exchanger: Cascaded Forward and Recurrent Models. *Eng* **2025**, *6*, 85. https://doi.org/10.3390/eng6050085

Copyright: © 2025 by the authors. Licensee MDPI, Basel, Switzerland. This article is an open access article distributed under the terms and conditions of the Creative Commons Attribution (CC BY) license (https://creativecommons.org/licenses/by/4.0/).

1. Introduction

The growing demand for energy efficiency in the industrial sector, driven by rising energy costs and the depletion of primary resources, has led to significant advancements in thermal management technologies. Heat exchangers, fundamental to processes such as power generation, chemical processing, and HVAC systems, play a crucial role in optimizing energy use. However, their performance is often hindered by fouling, which increases thermal resistance and reduces heat transfer efficiency. Overcoming these challenges is essential for improving system performance and ensuring long-term sustainability [1]. They are crucial for transferring thermal energy between fluids without mixing, significantly impacting the overall effectiveness of different systems [2].

The performance of heat exchangers is often affected by fouling. It is defined as the accumulation of unwanted substances or materials on one or both sides of the heat exchanger surface in various forms: sediments, crystals, biological residues, reaction byproducts, or a combination of these elements [3]. There are generally various causes that contribute to the development of deposits, such as the fouling mechanism and the composition of the fluid. Fouling decreases heat transfer rates, obstructs fluid flow, causes the corrosion of material surfaces, and contaminates working fluids, thereby impacting efficiency and operation [4,5]. The financial repercussions of fouling affect all industries through increased spending on equipment, production losses due to downtime, maintenance costs for deposit removal, and higher consumption of fuel, water, and electricity [6]. The petrochemical sector is notably among the most impacted industries. Various methods, such as filtration and chemical treatments, have been successful in controlling the occurrence and accumulation of deposits [7]. Once fouling occurs, regular and systematic cleaning becomes essential. Finding the right balance for cleaning intervals is crucial; shorter intervals lead to higher production downtime costs, while longer intervals increase energy consumption and environmental impact [8]. Given these challenges, the shift from systematic to predictive maintenance is becoming increasingly essential.

Researchers are prioritizing the prediction of fouling, driving the exploration of various methods to enhance predictive capabilities [9,10]. Conventional approaches, including experiments and computational fluid dynamics (CFD) simulations, face limitations in terms of time and accuracy when predicting fouling effects [11]. In response, research institutes are increasingly turning to more suitable models, such as statistical modeling algorithms.

Artificial intelligence (AI) techniques, often referred to as black box models, are employed to analyze the non-linear dynamics of complex systems [12,13]. In a study by Xiao Zheng et al. [14], General Regression Neural Networks (GRNNs) and Random Forest (RF) were utilized to forecast the coefficients of heat transfer, with GRNN demonstrating superior accuracy and generalization compared to RF. Jyoti Prakash Panda et al. [15] investigated heat transfer in exchangers equipped with twisted tape inserts using polynomial regression, RF, and artificial neural network (ANN), concluding that ANN was the most effective approach. Anurag Kumra et al. [16] employed Support Vector Machines (SVMs) and ANN for predicting rates of heat transfer in wire-on-tube exchangers, finding that SVM outperformed other methods. Emad M.S. El-Said et al. [17] applied Random Vector Functional Link (RVFL), SVM, and other methods to evaluate the thermo–hydraulic performance of shell and tube exchangers, identifying RVFL as a dependable modeling technique. Gupta et al. [18] utilized a model of neural network combined with a genetic optimization to analyze the performance of a counter flow plate fin compact heat exchanger. Their study found that the neural network's simulated data closely matched the experimental results, with errors between 10 and 20%. Roy et al. [19] focused on evaluating the performance of tube and shell heat exchangers (STHX), analyzing thermal parameters such as exegetic

and energetic efficiencies, electrical power, factor of fouling, and cost using a Feedforward Backpropagation network (FFBN) algorithm.

Muthukrishnan et al. [20] proposed a technique of machine learning for modeling and simulating tube and shell heat exchangers with the use of the Support Vector Machine technique to predict performance. Cao Shengxian et al. [21] used LS-SVM and BP neural networks to predict the fouling resistance in the shell and tube exchangers, focusing on factors like pH and bacteria levels. Wen et al. [22] applied Partial Least Squares (PLS) and Support Vector Regression (SVR) to forecast fouling in plate heat exchangers, determining that SVR was more accurate than PLS. Emad M.S. El-Said et al. [23] explored algorithms such as Social Media Optimization (SMO), k-nearest neighbors (kNN), SVM, and RVFL to estimate outlet temperature and values of pressure drop, with RVFL showing the best performance. Cao Shengxian et al. [24] revealed that LS-SVM and BP neural networks achieved greater accuracy than classical prediction methods of cooling water bio-fouling resistance, using parameters like pH, conductivity, and bacteria count. Mohanty [25] determined the difference in temperature in a tube and shell heat exchanger and its efficiency using a fouling factor-based artificial neural network structured as 6-5-4-2. Sundar et al. [26] utilized deep learning to predict the fouling factor, compiling a database of 15,600 samples with input variables such as temperatures of inlet fluid, the flow rate ratio of fouled fluid to those under clean conditions, and the outlet temperatures for both gas and fluid. Kuzucanlı et al. [27] forecasted the overall coefficient of heat transfer and fouling resistance in plate heat exchangers, conducting a comparative analysis of multi-classification algorithms to identify the most accurate model using experimental data and employing K-fold cross-validation with Naïve Bayes, k-nearest neighbors (kNN), and decision tree algorithms. The dataset was collected through experiments, with varying flow rates and intake temperatures serving as input factors. Hosseini et al. [28] computed the factor of fouling using four artificial intelligence models, decision tree (DT), Gaussian Process Regression (GPR), Support Vector Regression, and Bagged Tree. The dataset was generated by trials, with input factors such as the operational time; temperature of the surface; the velocity, density, and temperature of the fluid; and the equivalent diameter chosen based on an analysis of Pearson's correlation. R. Harche et al. [29] developed Random Forest (RF) and Long Short-Term Memory (LSTM) to anticipate fouling in crude distillation unit preheat trains in petroleum refineries using historical data. Similarly, Al-Naser et al. [30] employed LSTM and ANN in a two-step technique to determine the fouling factor for a shell and tube heat exchanger, achieving high prediction accuracy. Oleg Ilyunin et al. [31] introduced an ANN method for predicting the coefficient of heat transfer over time during the operation of plate heat exchangers (PHEs) and identifying the point at which it reaches its minimum permissible value, enhancing training parameters with fuzzy logic and incorporating both industrial measurements and mathematical models.

This study introduces a novel approach for estimating fouling resistance in heat exchangers using two artificial intelligence models: cascaded forward network (CFN) and recurrent neural network (RN). The models are optimized with the Levenberg–Marquardt algorithm to achieve high accuracy while using a minimal number of input parameters. The key contributions of this work include:

- Efficient Model Design: the proposed models utilize only six input parameters, reducing complexity while maintaining accuracy.
- High-Precision Training: the Levenberg–Marquardt algorithm ensures rapid convergence and minimizes mean squared error (MSE).
- Robust Validation: the models' generalization ability is tested using external datasets.
- Correlation Analysis: the relationships between input variables and fouling resistance are thoroughly analyzed.

- Statistical Performance Evaluation: error metrics, absolute error histograms, and descriptive statistics provide insight into model reliability and accuracy.

The rest of this paper is organized as follows: Section 2 discusses the heat exchanger data and the proposed neural network topologies. Section 3 summarizes the experimental data from the training and testing periods. Section 4 discusses a statistical analysis that includes the connection between input variables, absolute error histograms, and descriptive statistics for generating errors and model accuracy. Finally, Section 5 offers key findings and recommendations for future research.

2. Materials and Methods

The U100 atmospheric distillation unit is the main Algiers refinery unit (Algeria), and its purpose is to fractionate crude oil into different finished products such as kerosene, diesel, fuel, LPG, and light and heavy solvents that can be used in the composition of marketable products and reused for one or more treatments. One of the three centrifugal pumps, P101, pumps the crude oil from the storage tanks at room temperature to the unit of atmospheric distillation, which then passes through the two circuits of the E101 battery (CBA and FED) [29]. The crude oil passes through the tube side of the battery where it is heated using the overhead reflux (RT), a mixture of light products from the top of the distillation column C101 at tray N°46.

After the initial heating stage, the crude oil enters the desalter unit (D110), where it is washed with treated water to remove impurities such as salts and other non-useful and even undesirable components. The oil then goes through the electrostatic desalter by adding treated water and caustic soda. The water that is treated is injected at the entrance of the E101 exchanger and at the entrance of the desalter, aiming to wash the crude oil and remove the salts present (as illustrated in Figure 1, where the treated water is directed into D110 before the oil continues further processing).

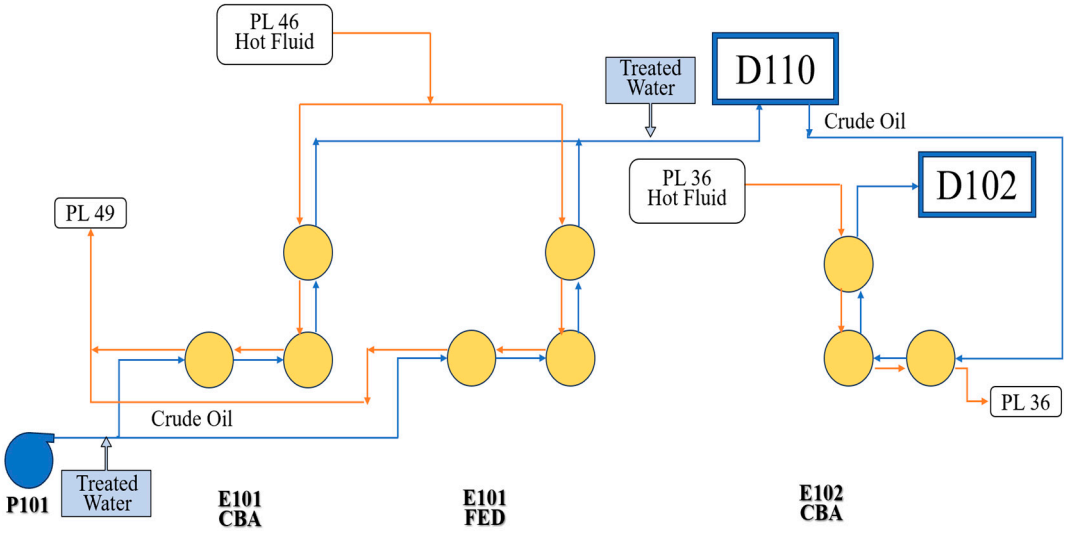


Figure 1. Diagrammatic representation of the crude oil preheating circuit in a simplified form.

After the desalination process, the crude oil then proceeds to the second stage of heat exchange in the E102 CBA additional exchanger, which further relies on the PL 36 hot fluid stream for heating. The heat exchanger's inlet and outlet temperatures for both fluids are measured at the extremities using four thermocouples. Simultaneously, the flow rates of crude oil and reflux are quantified at the heat exchanger's entrance utilizing flow meters. The control room supplies the relevant physical properties of the two fluids.

2.1. Experimental Procedure

This current study used data obtained from the heat exchanger cell E 101CBA (Figure 2), situated in the Algiers refinery's preheating circuit, spanning 290 days from 14 March 2019 to 17 December 2019. This cell comprises three counter-current shell-and-tube heat exchangers arranged in series. The characteristics of these exchangers are detailed in Tables 1 and 2.



Figure 2. The E101 CBA heat exchanger [32].

Table 1. Construction materials of heat exchanger E101 CBA.

Construction Material	**Carbon Steel**
Shell Diameter (m)	1.067
Baffle Spacing (m)	0.465
Number of Shells	3.000
Tube Outer Diameter (m)	0.020
Tube Thickness (m)	BGW14
Tube Length (m)	5.740
Total Number of Tubes	6600.000
Pitch: Staggered (m)	0.025
Total Heat Exchange Surface Area (m^2)	2322.770
Overall Heat Transfer Coefficient (kW/m^2 °C)	36.680

Table 2. Operating conditions of heat exchanger E101 CBA.

Parameter	**Shell Side**	**Tube Side**
Circulating Fluid	Head Reflux	Crude Oil
Mass Flow Rates (kg/s)	126.000	90.120
Viscosity (m^2/s) Inlet/Outlet	-	2.4×10^{-6}–9.6×10^{-7}
Inlet Temperature (K)	388.706	299.817
Outlet Temperature (K)	338.706	377.594
Number of Passes	1.000	4.000
Fouling Factor	0.001	0.002

The parametric range of operating variables corresponding to the heat exchanger used in this study is listed in Table 3. These variables are the inputs of the proposed models and are shown in Figure 3.

Table 3. Parametric range of variables (the inputs of the proposed models).

Variables	Symbol	Range
Inlet Temperature of Crude Oil (°C)	te	13–30
Outlet Temperature of Crude Oil (°C)	ts	94–119
Inlet Temperature of Head Reflux (°C)	Te	108.42–127.6
Outlet Temperature of Head Reflux (°C)	Ts	54–84
Mass Flow Rate of Crude Oil (kg/s)	$\dot{m}t$	111.6–439.2
Mass Flow Rate of Head Reflux (kg/s)	$\dot{m}c$	127.73–499

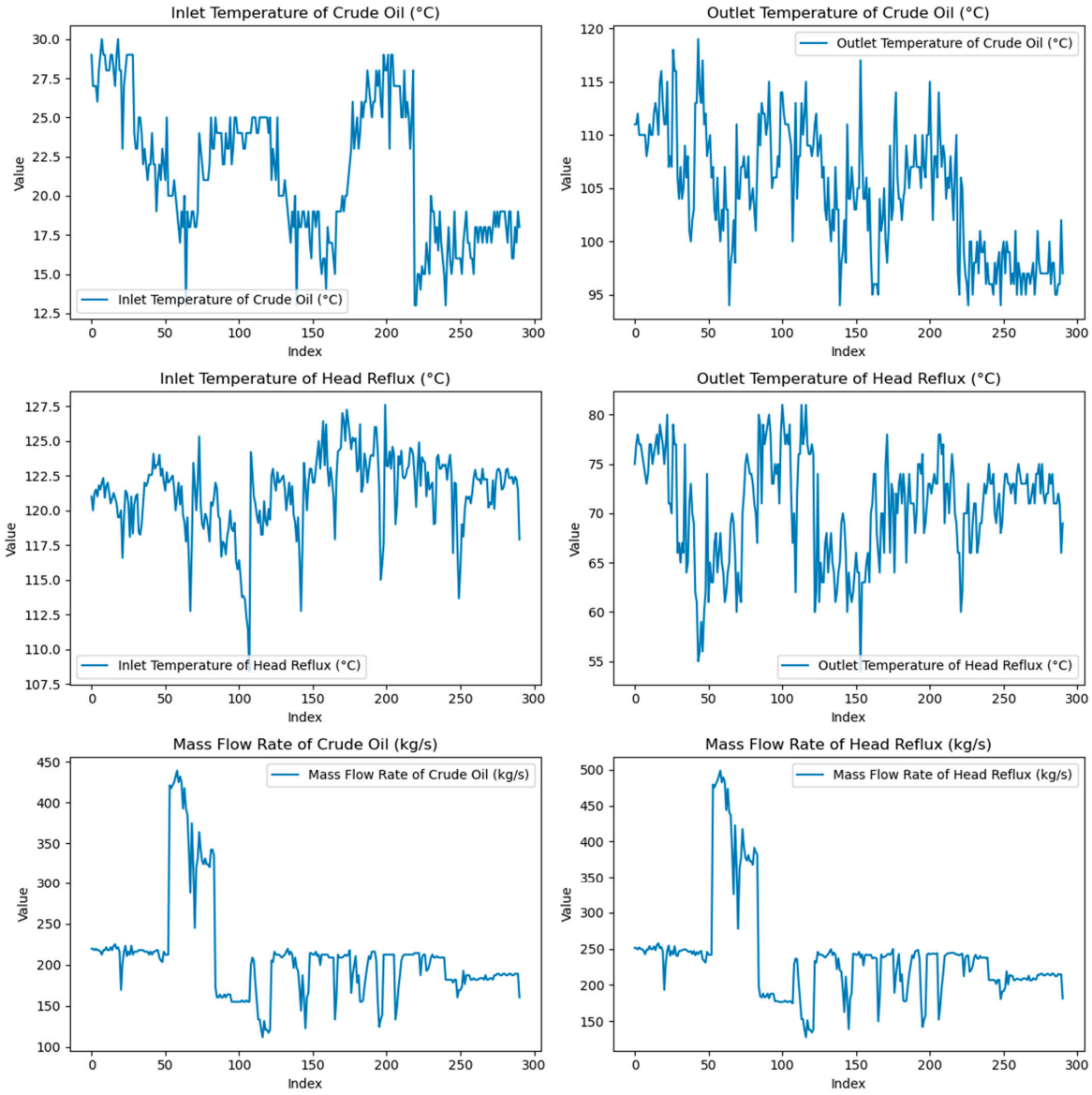


Figure 3. The parametric range of variables that are the inputs of the proposed artificial intelligence models.

To further demonstrate the results of this study, a subset of the raw experimental data is presented in Table 4. This subset contains operational data such as inlet and outlet temperatures associated with the heat exchangers, crude oil and treated water flow rates,

and pressure levels at specific locations in the system. The sample data provided are intended to serve as an illustration for the empirical part of this study and to help validate the accuracy of the proposed model. These values were selected for specific operational conditions to ensure that the predictive model captures reasonable modifications of the process parameters. In doing so, this study increases transparency, while the full dataset is available for validation if required, thereby improving reproducibility.

Table 4. Sample raw experimental data.

Row	te	ts	Te	Ts	ṁt	ṁc
1	29.00	111.00	121.00	75.00	219.60	251.29
2	27.00	111.00	120.00	77.00	219.60	251.03
3	27.00	112.00	121.25	78.00	217.80	249.24
4	27.00	110.00	121.50	77.00	219.60	251.91
5	26.00	110.00	121.00	77.00	217.80	249.71
6	28.00	110.00	121.80	76.00	217.80	249.49
7	29.00	110.00	121.50	75.00	216.00	247.11
8	30.00	110.00	122.00	74.00	212.40	242.44
9	29.00	108.00	122.33	73.00	217.80	248.82
10	29.00	109.00	120.90	74.00	217.80	248.66
...	...	...	...	...	...	...
291	18.00	97.00	117.90	69.00	160.20	181.29

2.2. Neural Networks Structures

This section provides a detailed discussion of the proposed neural network structure for data processing models, as illustrated in Figure 4. The proposed model structure includes two neural network approaches, namely the cascaded forward network and the recurrent network, which are used to predict the fouling resistance of a heat exchanger based on a set of inputs. The inputs used in both models consist of parameters related to the thermal system, including te (°C), which is the crude oil inlet temperature ranging from 13 °C to 30 °C; ts (°C), the crude oil outlet temperature ranging from 94 °C to 119 °C; Te (°C), the head reflux inlet temperature ranging from 108.42 °C to 127.6 °C; and Ts (°C), the head reflux outlet temperature, ranging from 54 °C to 84 °C. Additionally, there are two parameters related to mass flow rate, namely ṁt (kg/s), the crude oil mass flow rate, ranging from 111.6 to 439.2 kg/s, and ṁc (kg/s), the head reflux mass flow rate, ranging from 127.73 to 499 kg/s. Based on these input data, both neural networks aim to estimate the expected output, which is the fouling resistance (Rd), measured in square meters and degrees Celsius per watt (m^2 °C/W).

The cascaded forward network, as shown in Figure 4a, operates with a feedforward structure where each layer is directly connected only to the next layer, without any recurrent connections involving previous timesteps [33]. The input from the six mentioned parameters is processed through a hidden layer consisting of 15 neurons. Each neuron in the hidden layer is combined with weights (W) and biases (b) that allow for non-linear transformations. After the input passes through the hidden layer, the signal is processed by an activation function, producing the output from the hidden layer. The output from this hidden layer is then passed to the output layer, which consists of one neuron to generate a single output value at each time step. In this cascaded forward network, there is also a direct path from the input to the output layer, where some input information can directly influence the final result without passing through the hidden layer. This provides additional flexibility for the network to learn complex relationships between the input and output.

Meanwhile, the recurrent network in Figure 4b employs a different, more complex, and sophisticated approach as it involves recurrent connections. Like the cascaded forward

network, the input is fed into the network. However, what differentiates it is the recurrent connections in the hidden layer, which consists of 10 neurons. These recurrent connections allow for the network to retain information from the previous timestep, which is then used as additional input for the next timestep [34]. The weights and biases in the hidden layer, as in the forward model, are used to transform the input but with the added information from the previous time. The output from the hidden layer is then passed to the output layer, which, like in the cascaded forward network, consists of a single unit to generate one output value at each time step.

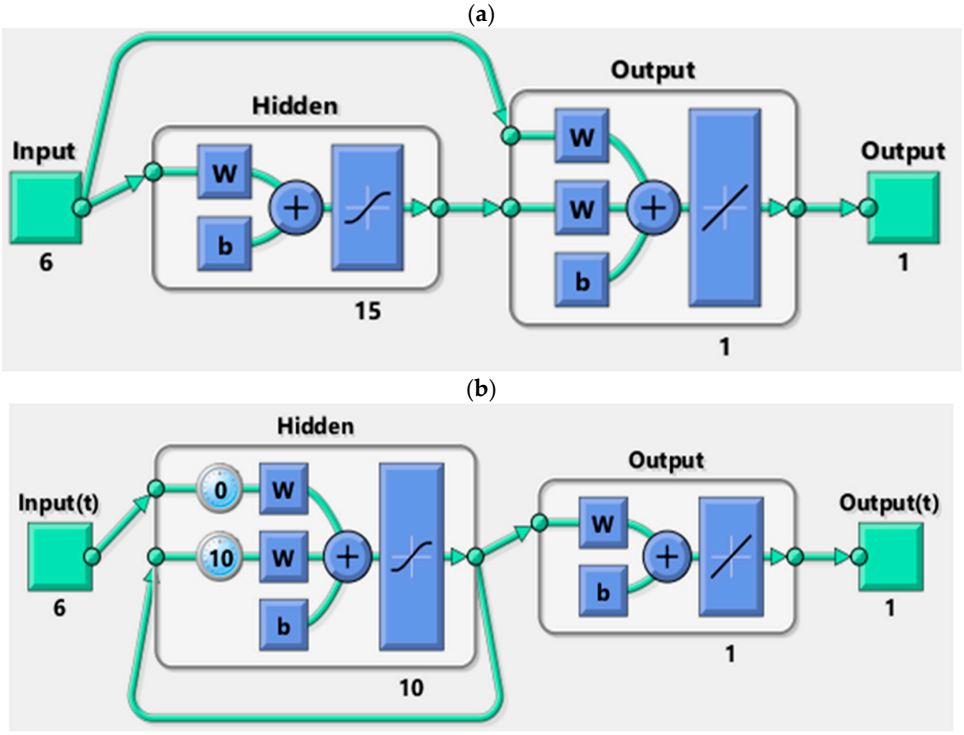


Figure 4. The structures of the proposed models. (**a**) Cascaded forward network structure, (**b**) recurrent network structure.

For both neural networks, the used activation functions for hidden and output layers are the tanh function.

The number of hidden neurons in each model is selected by trial and error experiments, as many different hidden neurons are carried out until the lowest mean squared error value (MSE) is obtained. This is because the main goal is to obtain the lowest value of the MSE.

3. Results

The first step in training and verifying the proposed model involves collecting data from the heat exchanger, which serves as an input for training the model. After the data are collected, the next step is to initialize the model parameters and select the number of hidden neurons in the hidden layer of the proposed neural network. The number of hidden neurons can affect the model's performance and its ability to capture complex patterns in the data. Once the parameters are initialized, the model is trained using the Levenberg–Marquardt (LM) algorithm, which is a second-order optimization algorithm used to speed up the convergence process in neural network training. At this stage, the model is trained to minimize the error between the predictions and the actual data. After training is completed, the model's performance is evaluated by checking whether the MSE is close to zero. If the MSE is still far from zero, the process returns to step three to adjust

the model parameters or change the number of hidden neurons used, and then the model is retrained to achieve a smaller error.

Once the MSE is sufficiently small, the research proceeds to the testing phase, where the trained model is tested. Testing is conducted using both the same data as used in training and different data to verify the model's generalization ability. At this stage, it is crucial to assess whether the training or approximation error is very small and close to zero. If the error is still too high, the process returns to step three for further adjustments to the model parameters and the neural network. However, if the error is very small and close to zero, the model is considered ready to be used for predicting fouling resistance in the heat exchanger. The methodology used to train and verify these models is illustrated in Figure 5.

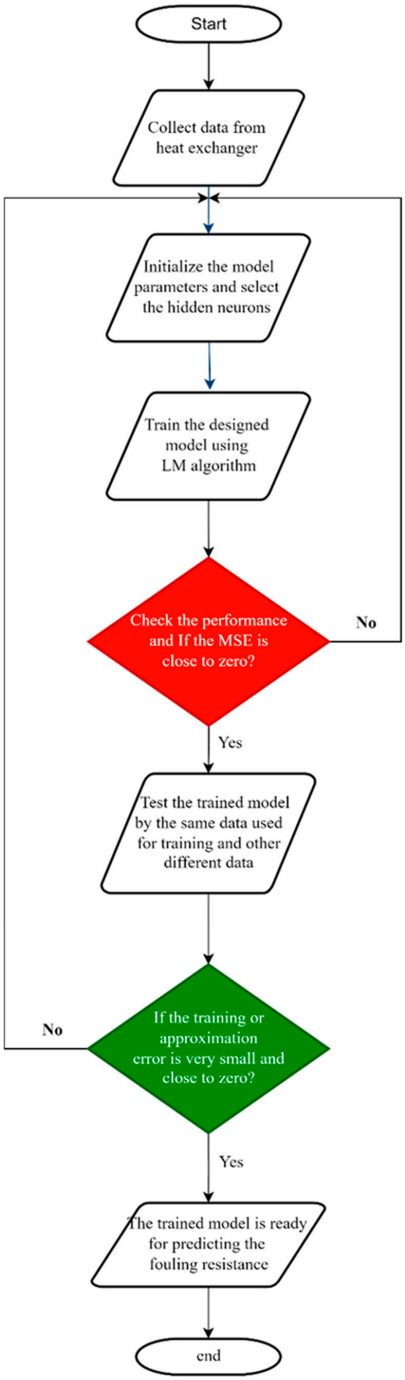
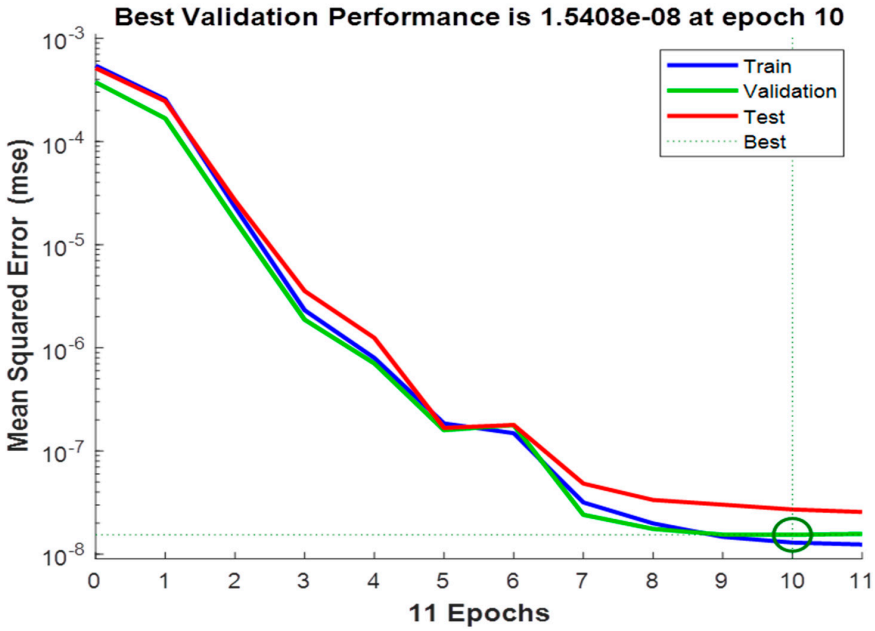


Figure 5. The methodology with the proposed models. Models are the cascaded forward and recurrent networks.

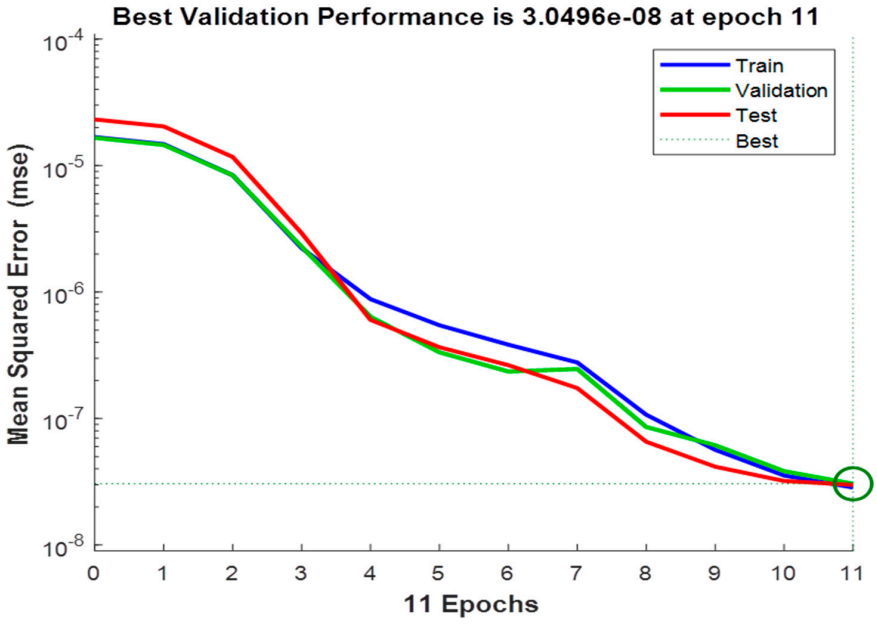
3.1. Results from Training Stage

The data are divided into three parts, as follows: 70% of the data were used for training, 15% for testing, and 15% for validation. The used algorithm for training is Levenberg–Marquardt (LM). The training process occurs using Intel(R) Core(TM) i5-8250U CPU @ 1.60 GHz 1.80 GHz.

For the cascaded forward network, the number of hidden neurons is 15 and the process of training is completed in 2 s. In the case of the recurrent network, the number of hidden neurons is 10 and the training is completed in 35 s. This means that the training using the cascaded forward network is faster. The hidden neurons mentioned are obtained after many trial and error experiments until the smallest MSE value is achieved. The results from the training process including the mean squared error (MSE) and the regression are shown in Figures 6 and 7.

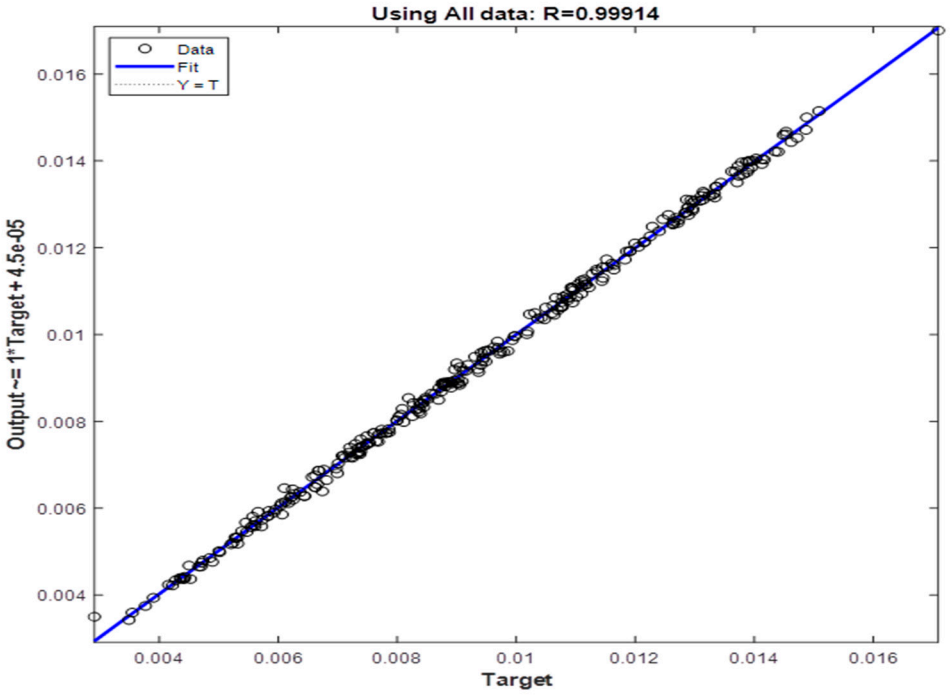


(**a**) The obtained MSE from the cascaded forward model.

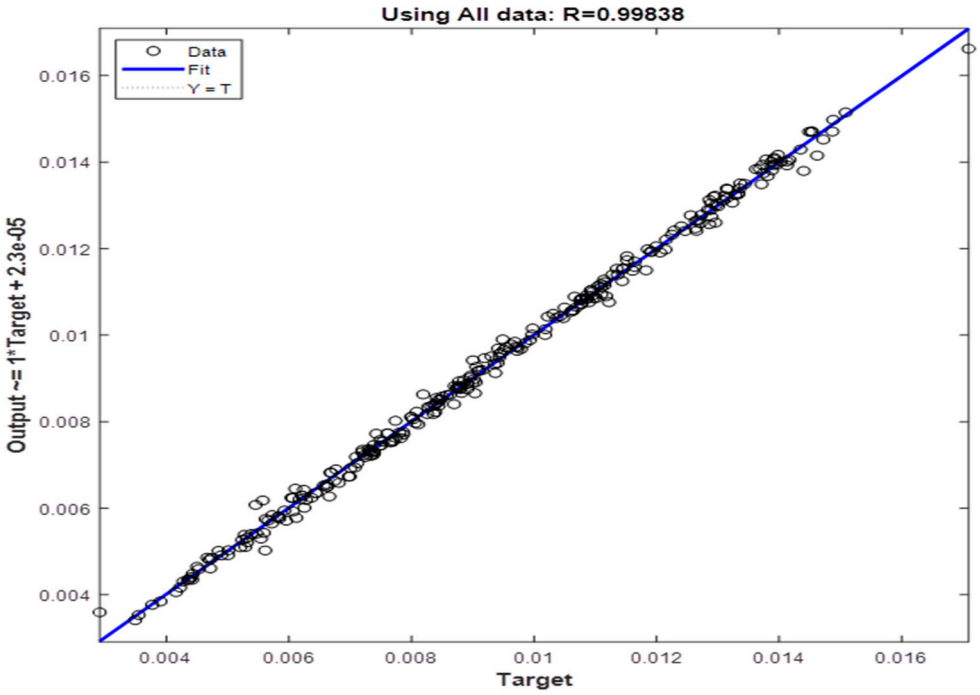


(**b**) The obtained MSE from the recurrent network model.

Figure 6. The obtained MSE from the proposed models.



(**a**) The obtained regression from the cascaded forward model.



(**b**) The obtained regression from the recurrent model.

Figure 7. The obtained regression (R) from the proposed models.

From Figure 6, the obtained MSE value is very small and close to zero in both models. This means that the models are trained efficiently. As can also be seen, the MSE using the cascaded forward model is 1.54×10^{-8}, which is smaller than the corresponding value of the recurrent model, which is 3.05×10^{-8}. This means that the cascaded forward model is the more accurate. From Figure 6, the regression value R is provided. The value R is very close to 1 in both models, which means that the estimated output by the model coincides with the actual output accurately. Using the cascaded forward model, the R value is 0.99914, which is larger than the corresponding value of the recurrent model. This proves that

the cascaded forward model has higher accuracy in estimating the fouling resistance of a heat exchanger.

3.2. Results from Verification Stage

In this section, the total amount of data is used to test and verify the effectiveness of the trained models. The comparison between the actual output and the estimated ones by the cascaded network and the recurrent network is presented in Figure 8. As can be seen, the estimated outputs coincide with the actual output, which means that the proposed models are efficient in estimating the fouling resistance correctly. The error values between these outputs are presented in Figure 9. Figure 9a shows the values of the real error (positive and negative sign) and Figure 9b shows the values of the absolute error (positive sign). As shown in Figure 9, the error or the absolute error is very small and close to zero using any model. This means that the proposed models are trained very well. The error that resulted from the cascaded network is lower than the error that resulted from the recurrent model. This means that the cascaded forward network has higher performance and accuracy. As presented in Figure 10, the average value of the error for the proposed models is calculated and compared. The average value of the error in the case of the cascaded forward is equal to 9.80446×10^{-5}, and the average value of the error in the case of the recurrent network is equal to 0.000126783. Therefore, this proves that the results obtained by the cascaded forward network are the best.

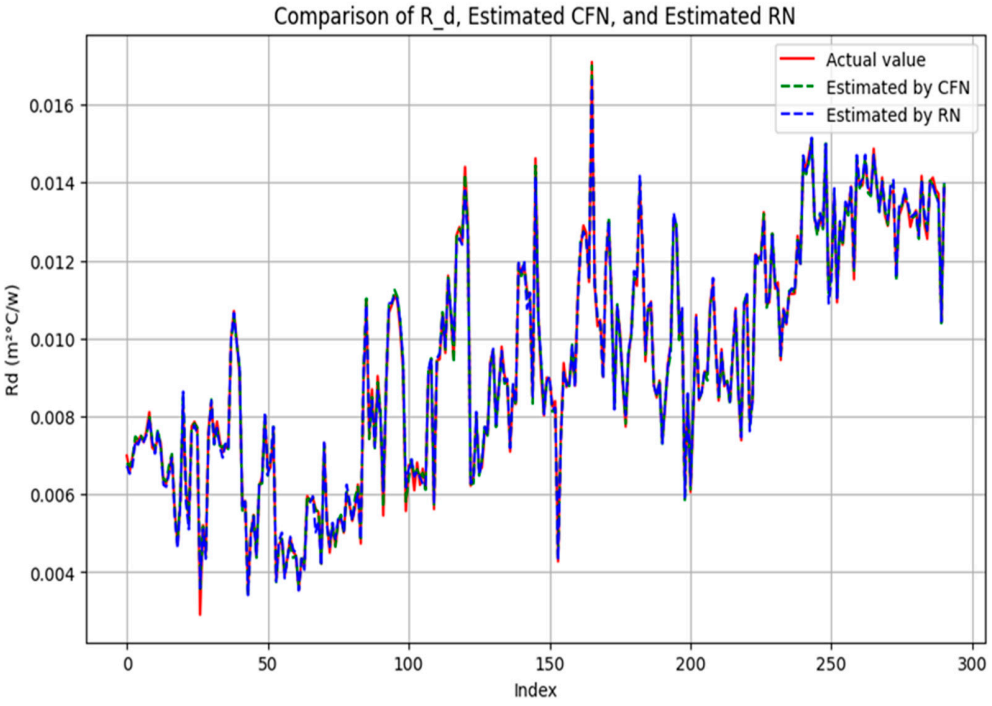
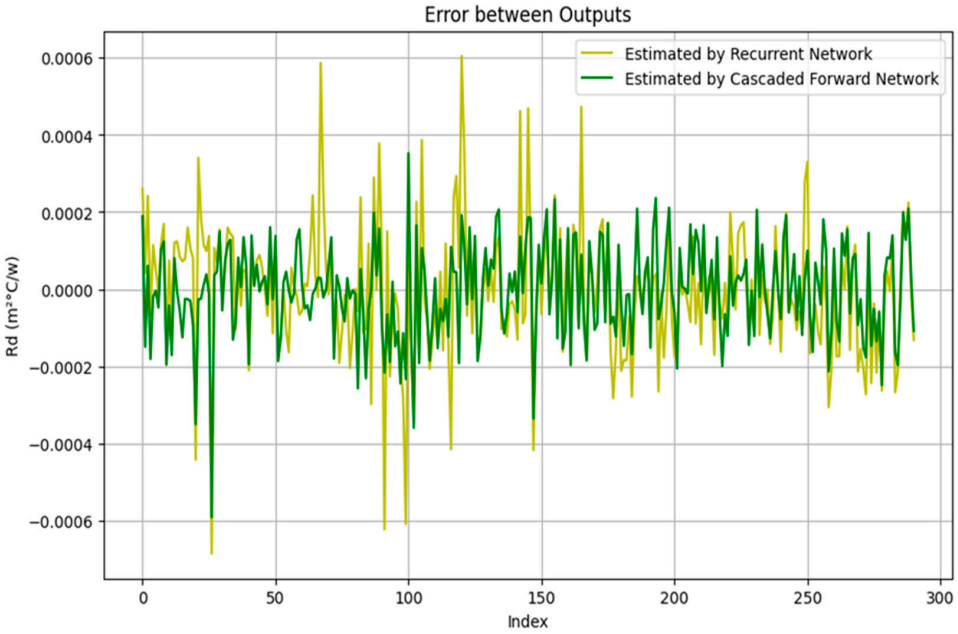


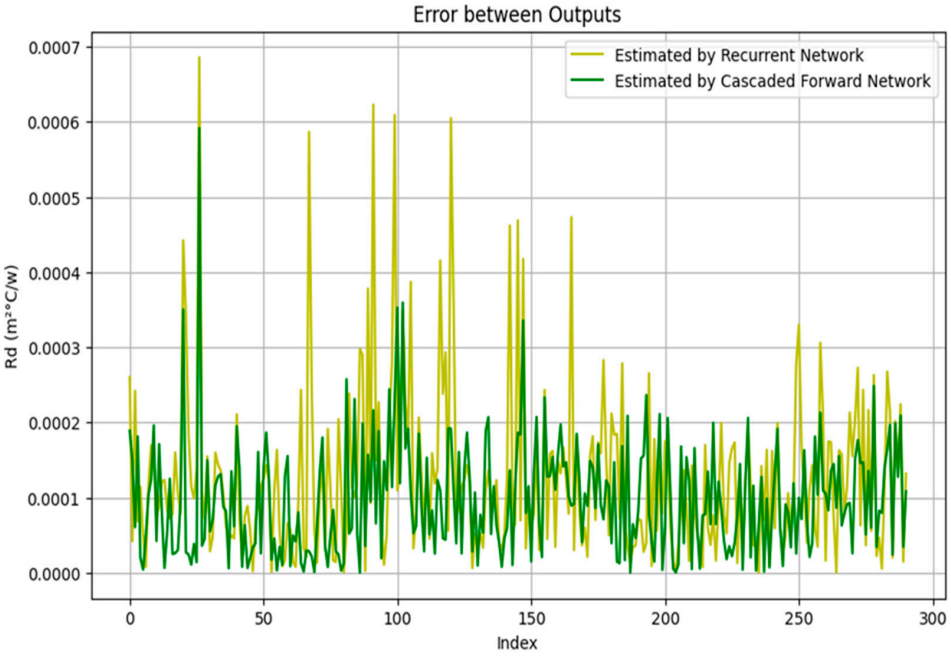
Figure 8. Comparing the outputs estimated by the proposed networks with the actual output. RN refers to the recurrent network model and CFN refers to the cascaded forward network.

Statistical Analysis of Performance Differences

To further assess the differences in performance between the two models, the standard deviation of errors was analyzed. The results show that CFN has a lower standard deviation (7.66×10^{-5}) compared to RN (1.14×10^{-4}), indicating that CFN provides more stable and reliable predictions. Furthermore, error histogram analysis reveals that CFN has a higher concentration of smaller errors, reinforcing its superior accuracy in estimating fouling resistance. Future work could include a formal statistical significance test, such as a paired t-test, to further validate these findings quantitatively.



(**a**) The real errors that resulted from proposed models (positive and negative signs).



(**b**) The absolute errors that resulted from proposed models (only positive sign).

Figure 9. Comparing the resulting errors by the proposed networks. The error is the difference between actual output and the estimated one.

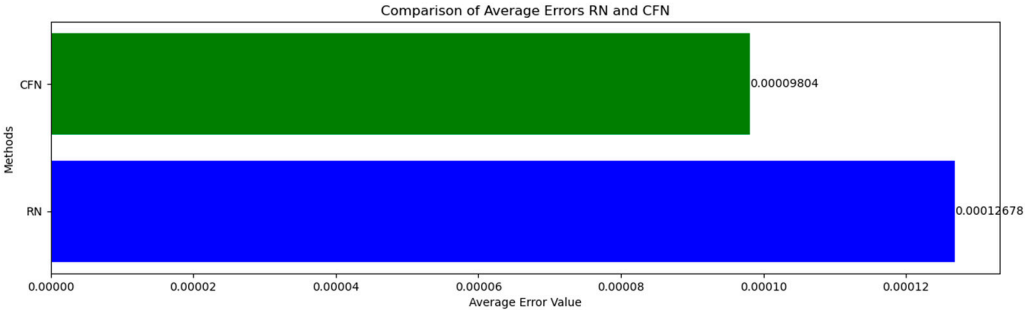


Figure 10. Comparing the average error rate of the proposed models. RN refers to the recurrent network model and CFN refers to the cascaded forward network.

4. Discussion

4.1. Correlation Between Input Variables

The correlation between the input variables of the proposed models is presented in Figure 11. Based on the correlation matrix displayed in Figure 11, there is a complex relationship between the variables related to the thermal efficiency of the system, represented by the output Rd (m^2 °C/w). The inlet temperature of crude oil (te) has a moderate negative correlation with Rd, reaching −0.428. This indicates that an increase in the inlet temperature of crude oil tends to decrease the thermal efficiency of the system. On the other hand, the outlet temperature of crude oil (ts) shows a stronger negative correlation with Rd, at −0.694, suggesting that an increase in outlet temperature significantly reduces thermal efficiency. This demonstrates that temperature management at both points, at the inlet and outlet, is crucial, as higher outlet temperatures correspond to lower achieved thermal efficiency.

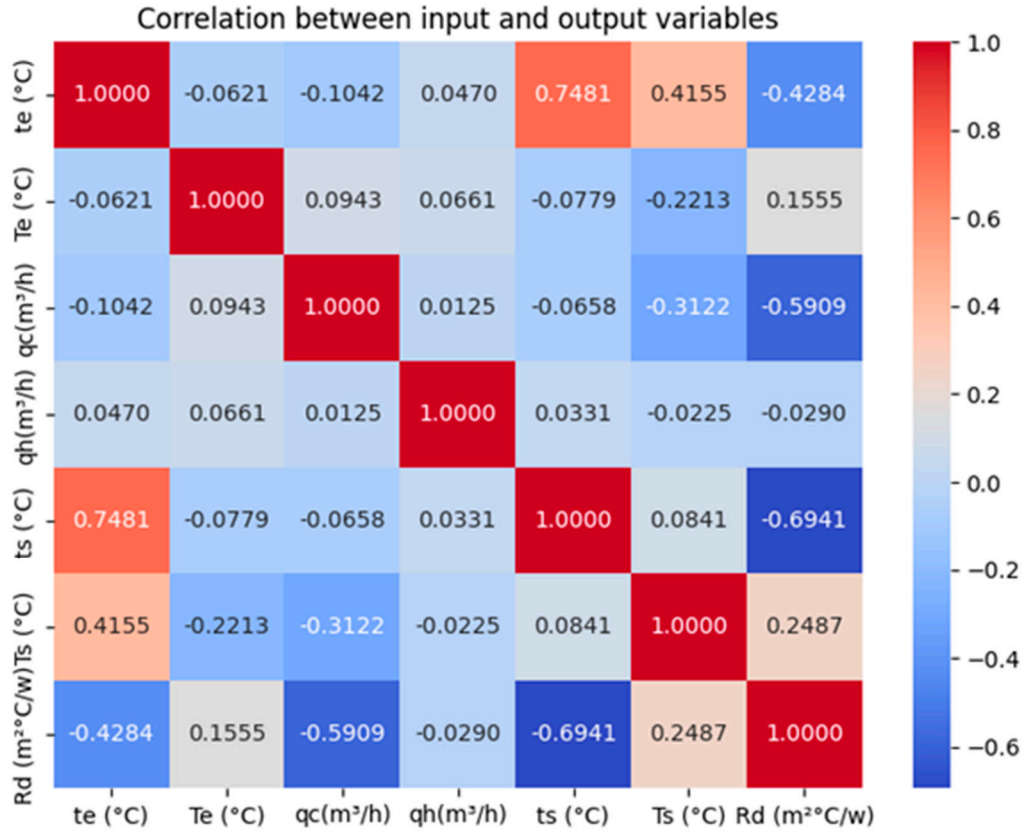


Figure 11. Correlation between the input variables of the proposed models.

Meanwhile, the inlet temperature of the head reflux (Te) shows a weak positive correlation with a Rd of 0.155. This indicates that although there is a relationship between the inlet temperature of head reflux and thermal efficiency, its impact is not significant. Conversely, the outlet temperature of the head reflux (Ts) has a clearer positive correlation with a Rd of 0.249. This suggests that an increase in the outlet temperature of the head reflux can contribute to thermal efficiency, even though its influence is not as strong as that of the other variables. The increase in temperature at this outlet point can help maintain process efficiency, highlighting the importance of temperature control at the head reflux outlet.

Furthermore, the correlation between the mass flow rate of crude oil ($\dot{m}t$) and the mass flow rate of head reflux ($\dot{m}c$) with Rd shows differing trends. The mass flow rate of crude oil tends to have a weaker influence on thermal efficiency, while the mass flow rate of head reflux exhibits a more significant negative relationship with Rd and may contribute to a

decrease in the system's thermal efficiency. This suggests that managing the flow rates, particularly from the head reflux, can have important implications for overall thermal performance and that balancing these variables is critical for achieving optimal thermal efficiency in the process.

4.2. Error Histogram

The histogram of the absolute errors that resulted from the proposed models is shown in Figure 12. The histogram analysis for errors by the recurrent network shows that many errors are distributed within a very small range of values. The first bin, which covers a range from approximately 2.78×10^{-7} to 6.88×10^{-5}, records the highest number of occurrences at 103. This indicates that many predictions are very close to the actual values, reflecting the good performance of the recurrent network model in terms of accuracy. The frequency of errors remains high in the second (85) and third bins (56), suggesting that while errors do occur, they still fall within a relatively small range. However, as we move to larger bins, there is a significant decrease in frequency, with only 10 occurrences in the fifth bin and even fewer in the others. This indicates that larger errors are rare, demonstrating the stability of the model.

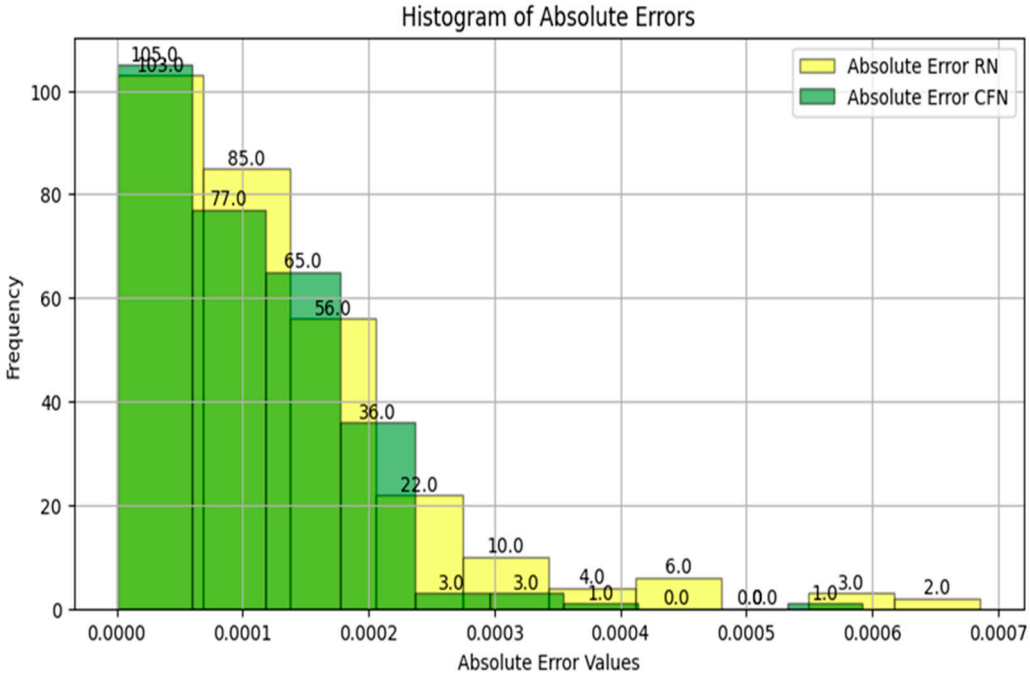


Figure 12. Histogram of the absolute errors resulting from the proposed models. RN refers to the recurrent network model and CFN refers to the cascaded forward network.

On the other hand, the histogram for error by the cascaded forward network exhibits a similar distribution pattern but with some significant differences. The first bin in the cascaded forward histogram records 105 occurrences, slightly higher than the error from the recurrent network, indicating that the cascaded forward network model also performs well, with many predictions close to the actual values. However, despite maintaining high numbers in the second (77) and third (65) bins, there is a sharper decline in the fourth bin, with only 36 occurrences, and there are significantly fewer in the higher bins. The fifth bin and beyond show very low frequencies (only three or one), suggesting that larger errors are quite rare in this model. When comparing these two histograms, it is evident that although both models exhibit a concentration of errors approaching zero, the cascaded forward network appears to be slightly superior in terms of accuracy, with more occurrences of small error values.

4.3. Descriptive Statistical Analysis

The descriptive statistical analysis of the absolute errors from the recurrent network and cascaded forward network, as presented in Figure 13, provides valuable insights into the performance of each model. For the recurrent network model, 291 measurements were analyzed, yielding an average absolute error of 1.27×10^{-4} and a standard deviation of 1.14×10^{-4}, indicating considerable variability in these errors. The minimum absolute error recorded was 2.78×10^{-7}, while the maximum reached 6.86×10^{-4}, signifying instances of highly inaccurate predictions. Most errors were distributed between the first quartile (25% at 5.01×10^{-5}) and the third quartile (75% at 1.64×10^{-4}), suggesting that around 50% of the error values cluster around 1.04×10^{-4}. This indicates that despite some extreme values, most errors are relatively small.

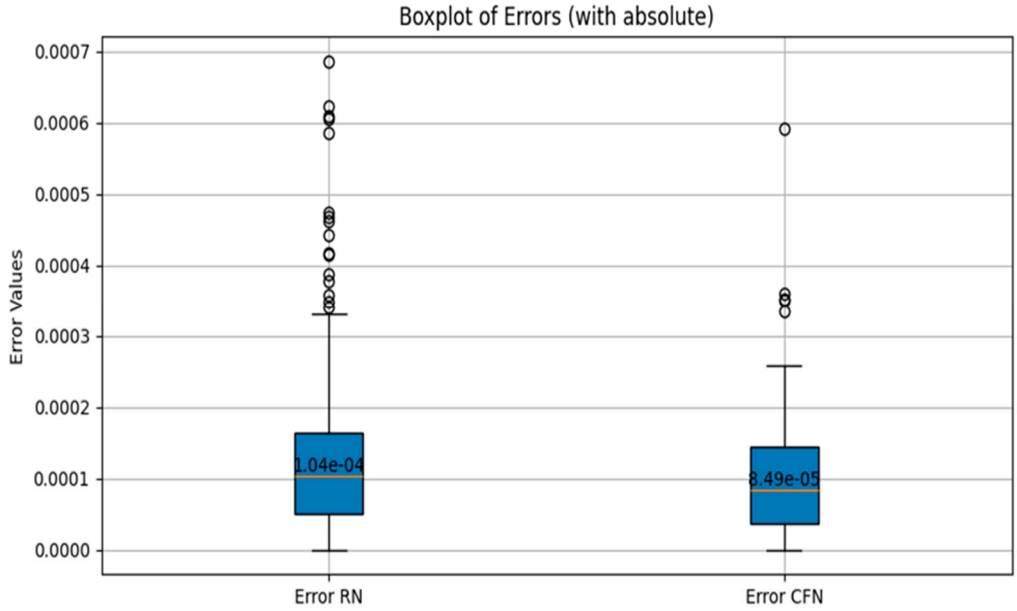


Figure 13. The descriptive statistical analysis (boxplot) of the absolute errors resulting from the proposed models. RN refers to the recurrent network model and CFN refers to the cascaded forward network.

On the other hand, the cascaded forward network model demonstrates slightly better statistics, with a lower average absolute error of 9.80×10^{-5} compared to the recurrent network, and a smaller standard deviation (7.66×10^{-5}), indicating a more even distribution of errors and lower variability. The minimum absolute error for the cascaded forward network is also smaller (1.93×10^{-7}), while the maximum reaches 5.92×10^{-4}. The first and third quartiles of the cascaded forward network show that 50% of the errors fall within a range of 8.49×10^{-5}, reflecting more accurate performance.

4.4. Comparison with Other Models

Indicating its originality and relevance. Table 5 presents a comparison with previous research that aligns closely with this current study, particularly in terms of input parameters. The studies selected for comparison focus on predicting heat exchanger fouling. From this analysis, it becomes evident that the cascaded forward network (CFN) and the recurrent neural network (RN) stand out as the most accurate and reliable models, especially when considering their ability to predict values related to heat exchanger fouling.

Table 5. Predicted fouling resistance comparison with previous studies.

Refs.	Prediction Variable	Model Type	Evaluation Index
Tong et al. [35]	Ash fouling resistance	Support Vector Machine (SVM)	R = 0.985
Davoudi and Vaferi. [14]	Fouling resistance in heat exchanger	Artificial Neural Network with MLP	R^2 = 0.978
Hossain et al. [28]	Fouling factor	Gaussian Process Regression (GPR)	R^2 = 0.988
Jradi et al. [36]	Fouling Resistance	Artificial Neural Network (ANN)	R^2 = 0.994
Present work	Fouling resistance	Cascaded forward network (CFN) and the recurrent neural network (RN)	R = 0.999

These models have been highlighted for their superior performance, suggesting that their methodologies could serve as valuable benchmarks in predictive modeling within similar fields. Comparing these models provides useful insights into the strengths and potential areas of improvement for the current research approach, further validating its significance in the context of the broader scientific community.

5. Conclusions and Future Work

In this paper, the fouling resistance of the heat exchanger is predicted using the cascaded forward neural network and the recurrent neural network. The models are built using six inputs to minimize their complexity. To train the built models, a fast algorithm is used, which is the Levenberg–Marquardt algorithm. The training process is carried out quickly and the smallest MSE value is obtained in each model. In each model, the MSE value is close to zero and the cascaded forward network has a smaller MSE value. This proves that both models are accurate and the cascaded network is the better. For testing the trained models, the training and other different data are used and the error and its absolute value are determined. The results from this stage reveal that both models provide few errors and are accurate. In addition, the accuracy of the cascaded forward network is better. A statistical analysis of the results was carried out, And the result from this analysis proves that there is a relationship between the input variables and the output, which is the fouling resistance. Furthermore, the cascaded forward network appears to be slightly superior in terms of accuracy.

Future work can include using other different neural networks and deep learning approaches. In addition, other machine learning techniques and training algorithms can be investigated. Incorporating hybrid AI models or real-time predictive maintenance integration can also be investigated. Furthermore, further refinement of the development with the integration of other sensor inputs, such as pressure or chemical composition, could improve the accuracy of the predictions. These variables could lead to a better understanding of the thermodynamic and chemical processes occurring in the system, which could improve the accuracy of the model. The development of techniques for multi-modal data fusion that can integrate data from multiple sensors could further improve the predictive power.

Author Contributions: Conceptualization, I.K., A.D. and A.-N.S.; methodology, I.K., A.D., A.M. and A.-N.S.; software, A.-N.S., F.F. and A.M.; validation, I.K., A.D., A.A.M. and A.-N.S.; formal analysis, F.F., A.M., A.A. and A.-N.S.; investigation, A.-N.S., I.K., A.A.M. and F.F.; resources, I.K., A.D., L.M. and A.-N.S.; data curation, I.K. and A.D.; writing—original draft preparation, A.-N.S., I.K. and A.D.; writing—review and editing, A.-N.S., A.A.M. and A.A.; Supervision: A.A. and L.M.; Project administration: L.M. All authors have read and agreed to the published version of the manuscript.

Funding: This research received no external funding.

Institutional Review Board Statement: Not applicable.

Informed Consent Statement: Not applicable.

Data Availability Statement: Data will be made available upon request to the first author.

Conflicts of Interest: The authors declare no conflicts of interest.

References

1. Olympios, A.V.; McTigue, J.D.; Farres-Antunez, P.; Tafone, A.; Romagnoli, A.; Li, Y.; Ding, Y.; Steinmann, W.-D.; Wang, L.; Chen, H.; et al. Progress and prospects of thermo-mechanical energy storage—A critical review. *Prog. Energy* **2021**, *3*, 22001. [CrossRef]
2. Tavousi, E.; Perera, N.; Flynn, D.; Hasan, R. Heat transfer and fluid flow characteristics of the passive method in double tube heat exchangers: A critical review. *Int. J. Thermofluids* **2023**, *17*, 100282. [CrossRef]
3. Roy, U.; Majumder, M. Economic optimization and energy analysis in shell and tube heat exchanger by meta-heuristic approach. *Vacuum* **2019**, *166*, 413–418. [CrossRef]
4. Delrot, S.; Guerra, T.M.; Dambrine, M.; Delmotte, F. Fouling detection in a heat exchanger by observer of, Takagi-Sugeno type for systems with unknown polynomial inputs. *Eng. Appl. Artif. Intell.* **2012**, *25*, 1558–1566. [CrossRef]
5. Musawel, R.K. Simulation and Fouling Study of Propane Heat Exchangers. Master's Thesis, University of Basrah, Basrah, Iraq, 2002.
6. Coletti, F.; Hewitt, G. *Crude Oil Fouling: Deposit Characterization, Measurements, and Modeling*; Gulf Professional Publishing: Woburn, MA, USA, 2014.
7. Diaz-Bejarano, E.; Behranvand, E.; Coletti, F.; Mozdianfard, M.R.; Macchietto, S. Organic and inorganic fouling in heat exchangers: Industrial case study analysis of fouling rate. *Ind. Eng. Chem. Res.* **2018**, *58*, 228–246. [CrossRef]
8. Al Hadad, W.; Schick, V.; Maillet, D. Fouling detection in a shell and tube heat exchanger using variation of its thermal impulse responses: Methodological approach and numerical verification. *Appl. Therm. Eng.* **2019**, *155*, 612–619. [CrossRef]
9. Das, S.; O'Connell, M.G.; Xu, H.; Bernstein, R.; Kim, J.-H.; Sankhala, K.; Segal-Peretz, T.; Shevate, R.; Zhang, W.; Zhou, X.; et al. Assessing advances in anti-fouling membranes to improve process economics and sustainability of water treatment. *ACS EST Eng. J.* **2022**, *2*, 2159–2173. [CrossRef]
10. Ikram, K.; Djilali, K.; Abdennasser, D.; Al-Sabur, R.; Ahmed, B.; Sharkawy, A.-N. Comparative analysis of fouling resistance prediction in shell and tube heat exchangers using advanced machine learning techniques. *Res. Eng. Struct. Mater.* **2023**, *10*, 253–270. [CrossRef]
11. Berce, J.; Zupančič, M.; Može, M.; Golobič, I. Infrared thermography observations of crystallization fouling in a plate heat exchanger. *Appl. Therm. Eng.* **2023**, *224*, 120116. [CrossRef]
12. Fawait, A.B.; Rahmah, S.; da Costa, A.D.S.; Insyroh, N.; Firdaus, A.A. Implementation of Data Mining Using Simple Linear Regression Algorithm to Predict Export Values. *Sci. J. Eng. Res.* **2025**, *1*, 26–32.
13. Sharkawy, A.N. Principle of neural network and its main types. *J. Adv. Appl. Comput. Math.* **2020**, *7*, 8–19. [CrossRef]
14. Davoudi, E.; Vaferi, B. Applying artificial neural networks for systematic estimation of degree of fouling in heat exchangers. Chem. *Eng. Res. Des.* **2018**, *130*, 138–153. [CrossRef]
15. Ben-Mansour, R.; El-Ferik, S.; Al-Naser, M.; Qureshi, B.A.; Eltoum, M.A.M.; Abuelyamen, A.; Al-Sunni, F.; Ben Mansour, R. Experimental/Numerical Investigation and Prediction of Fouling in Multiphase Flow Heat Exchangers: A Review. *Energies* **2023**, *16*, 2812. [CrossRef]
16. Zheng, X.; Yang, R.; Wang, Q.; Yan, Y.; Zhang, Y.; Fu, J.; Liu, Z. Comparison of GRNN and RF algorithms for predicting heat transfer coefficient in heat exchange channels with bulges. *Appl. Therm. Eng.* **2022**, *217*, 119263. [CrossRef]
17. Panda, J.P.; Kumar, B.; Patil, A.K.; Kumar, M.; Kumar, R. Machine learning assisted modeling of thermohydraulic correlations for heat exchangers with twisted tape inserts. *Acta Mech. Sin.* **2023**, *39*, 322036. [CrossRef]
18. Gupta, A.K.; Kumar, P.; Sahoo, R.K.; Sahu, A.K.; Sarangi, S.K. Performance measurement of plate fin heat exchanger by exploration: ANN, ANFIS, GA, and SA. *J. Comput. Des. Eng.* **2017**, *4*, 60–68. [CrossRef]
19. Roy, U.; Majumder, M. Evaluating heat transfer analysis in heat exchanger using, NN with, IGWO algorithm. *Vacuum* **2019**, *161*, 186–193. [CrossRef]
20. Muthukrishnan, S.; Krishnaswamy, H.; Thanikodi, S.; Sundaresan, D.; Venkatraman, V. Support vector machine for modeling and simulation of heat exchangers. *Therm. Sci.* **2020**, *24*, 499–503. [CrossRef]
21. Kumra, A.; Rawal, N.; Samui, P. Prediction of heat transfer rate of a, Wire-on-Tube type heat exchanger: An, Artificial, Intelligence approach. *Procedia Eng.* **2013**, *64*, 74–83. [CrossRef]
22. Wen, X.Q. Study on the methods of predicting the fouling characteristics of plate heat exchanger based on water quality parameters. *Appl. Mech. Mater.* **2013**, *459*, 153–158. [CrossRef]

23. El-Said, E.M.S.; Abd Elaziz, M.; Elsheikh, A.H. Machine learning algorithms for improving the prediction of air injection effect on the thermohydraulic performance of shell and tube heat exchanger. *Appl. Therm. Eng.* **2021**, *185*, 116471. [CrossRef]
24. Shengxian, C.; Yanhui, Z.; Jing, Z.; Dayu, Y. Experimental Study on Dynamic Simulation for Biofouling Resistance Prediction by Least Squares Support Vector Machine. *Energy Procedia* **2012**, *17*, 74–78. [CrossRef]
25. Mohanty, D.K. Application of neural network model for predicting fouling behaviour of a shell and tube heat exchanger. *Int. J. Ind. Syst. Eng.* **2017**, *26*, 228. [CrossRef]
26. Sundar, S.; Rajagopal, M.C.; Zhao, H.; Kuntumalla, G.; Meng, Y.; Chang, H.C.; Shao, C.; Ferreira, P.; Miljkovic, N.; Sinha, S.; et al. Fouling modeling and prediction approach for heat exchangers using deep learning. *Int. J. Heat Mass Transf.* **2020**, *159*, 120112. [CrossRef]
27. Kuzucanlı, S.A.; Vatansever, C.; Yaşar, A.E.; Karadeniz, Z.H. Assessment of fouling in Plate Heat exchangers using classification machine learning algorithms. In Proceedings of the CLIMA 2022 The 14th REHVA HVAC World Congress, Rotterdam, The Netherlands, 22–25 May 2022. [CrossRef]
28. Hosseini, S.; Khandakar, A.; Ayari, M.A.; Rahman, T.; Chowdhury, M.H.; Vaferi, B. Novel and robust machine learning approach for estimating the fouling factor in heat exchangers. *Energy Rep.* **2022**, *8*, 8767–8776. [CrossRef]
29. Harche, R.; Mouheb, A. The fouling in the crude distillation preheat train of Algerian refinery. *Acta Period. Technol.* **2022**, *53*, 272–284. [CrossRef]
30. Al-Naser, M.; El-Ferik, S.; Ben Mansour, R.; AlShammari, H.Y.; AlAmoudi, A. Intelligent Prediction Approach of Fouling Location in Shell and Tube Heat Exchanger. In Proceedings of the 2020 IEEE 10th International Conference on System Engineering and Technology (ICSET), Shah Alam, Malaysia, 9 November 2020; pp. 139–144. [CrossRef]
31. Ilyunin, O.; Bezsonov, O.; Rudenko, S.; Serdiuk, N.; Udovenko, S.; Kapustenko, P.; Arsenyeva, O. The neural network approach for estimation of heat transfer coefficient in heat exchangers considering the fouling formation dynamic. *Therm. Sci. Eng. Prog.* **2024**, *51*, 102615. [CrossRef]
32. Harche, R.; Mouheb, A.; Absi, R. The fouling in the tubular heat exchanger of Algiers refinery. *Heat Mass Transf.* **2016**, *52*, 947–956. [CrossRef]
33. Sharkawy, A.N.; Ameen, A.G.; Mohamed, S.; Abdel-Jaber, G.T.; Hamdan, I. Design, assessment, and modeling of multi-input single-output neural network types for the output power estimation in wind turbine farms. *Automation* **2024**, *5*, 190–212. [CrossRef]
34. Sharkawy, A.N.; Ali, M.M.; Mousa, H.H.; Ali, A.S.; Abdel-Jaber, G.T.; Hussein, H.S.; Ismeil, M.A. Solar PV power estimation and upscaling forecast using different artificial neural networks types: Assessment, validation, and comparison. *IEEE Access* **2023**, *11*, 19279–19300. [CrossRef]
35. Tong, S.; Zhang, X.; Tong, Z.; Wu, Y.; Tang, N.; Zhong, W. Online ash fouling prediction for boiler heating surfaces based on wavelet analysis and support vector regression. *Energies* **2019**, *13*, 59. [CrossRef]
36. Jradi, R.; Marvillet, C.; Jeday, M.R. Application of an artificial neural networks method for the prediction of the tube-side fouling resistance in a shell-and-tube heat exchanger. *Fluid Dyn. Mater. Process.* **2022**, *18*, 1511–1519. [CrossRef]

Disclaimer/Publisher's Note: The statements, opinions and data contained in all publications are solely those of the individual author(s) and contributor(s) and not of MDPI and/or the editor(s). MDPI and/or the editor(s) disclaim responsibility for any injury to people or property resulting from any ideas, methods, instructions or products referred to in the content.